# Specifics of solvation of sulfonated polyelectrolytes in water, dimethylmethylphosphonate, and their mixture: A molecular simulation study

Aleksey Vishnyakov and Alexander V. Neimark[a)]
*Department of Chemical and Biochemical Engineering, Rutgers, The State University of New Jersey, 98 Brett Road, Piscataway, New Jersey 08854, USA*

(Received 24 December 2007; accepted 26 February 2008; published online 22 April 2008)

Sulfonated polyelectrolyte membranes (PEMs), such as Nafion and styrene-olefin block copolymers, are explored as permselective membranes for fuel cells as well as suitable barrier materials against chemical agents. The permselective properties of PEM are determined by their microphase segregation into hydrophilic and hydrophobic domains. We performed classical molecular dynamics simulations of solvation of the hydrophilic fragments of PEM exemplified on sulfonated polystyrene (sPS) with potassium, calcium, and aluminum as counterions, in water, phosphor-organic nerve agent simulant dimethylmethylphosphonate (DMMP), and their binary mixture. The force field for the sulfonate group has been developed by optimizing the potential parameters to fit the benzenesulfonate conformations obtained from the density functional theory. For a comparison, we considered perfluorosulfonate oligomers representing fragments of Nafion polymer. We found a noticeable difference between the geometries of the polymer backbone in different solvents. The polymer backbone is stiffer in DMMP for both sPS and Nafion. An anisotropic structuring of the solvent around the phenylsulfonate group is substantially stronger than around the Nafion sidechain due to the rigidity and the anisotropy of the phenylsulfonate group. The counterion significantly affects the conformations of solvated sPS: the rigidity of the backbone increases when potassium or calcium ions are replaced by trivalent aluminum ions. © *2008 American Institute of Physics*.
[DOI: 10.1063/1.2899327]

## I. INTRODUCTION

The search for novel polyelectrolyte membranes (PEMs) suitable as permselective diffusion media is one of the key problems in the engineering of new fuel cell membranes and protective barriers.[1] Most experimental and simulation studies of PEM are related to Nafion and other perfluorosulfonate polymers. Recent theoretical and simulation works made a significant progress in (1) the development of molecular force fields for Nafion backbone and sidechain,[2–4] (2) *ab initio* and density functional theory (DFT) modeling of Nafion sidechain and its interactions with water,[5–9] (3) molecular mechanics and molecular dynamics (MD) atomistic modeling of the solvation of Nafion sidechains and polymer fragments in various solvents, such as water, methanol, water-methanol mixture, and nerve agent simulant dimethylmethylphosphonate (DMMP),[5,10] (4) MD simulations of nanoscale segregation and diffusion in hydrated Nafion membranes,[4,9,11–28] (5) modeling of the diffusion of water and ions in the vicinity of water-ionomer interfaces,[27,29–31] (6) the development of semiempirical models of proton conduction[14,15,26–28,32] (for reviews, see Refs. 33 and 34), and (7) the development of various regular and random network models.[35–37] Other simulation studies of polyelectrolytes on the atomistic level include molecular modeling of poly(ethyleneoxide)sulfonic acid in water,[38] MD modeling of counterion influence on DNA solvation in water,[39] and simulations of polyacrylic acid with calcium counterion.[40] Mesoscale approaches to polyelectrolyte modeling included dissipative particle dynamics,[41,42] self-consistent field theories,[43] integral equations,[44] cellular automata,[45] and solvent-free Monte Carlo techniques.[46–49] Hydration and water diffusion in sulfonated dendrimers grafted onto different backbone ionomers, including Nafion and sPS were recently modeled by Jang and Goddard.[4] The authors considered large (70–80 Å) systems and analyzed polymer structuring and water diffusion in the hydrated polymers. The mobility of water in sPS was lower than that in Nafion at the same water content.

This work was motivated by the prospective applications of PEM as permselective protective barriers. Due to the high water vapor permeability, outstanding chemical resistance, thermal stability, mechanical strength, and reduced weight, PEM opens new prospects for producing protective barriers with superior blocking and comfort properties.[1] A properly designed PEM may serve as a molecular sieve letting through water and blocking organic contaminants and biological agents.

PEM made of block copolymers, such as sulfonated styrene-olefin triblock copolymers, attracted considerable attention as low cost substitutes for Nafion type membranes. The important difference in solvent diffusion through perfluorosulfonate polymers of Nafion type and sulfonated tri-

a)Author to whom correspondence should be addressed. Electronic mail: aneimark@rutgers.edu.

 

block copolymers is rooted in their microstructure. Perfluorosulfonate polymers are generally insoluble in water.[50] When these polymers are exposed to water, water first aggregates in clusters around the hydrophilic sidechains; as the water content increases, the clusters coalesce into hydrophilic aggregates, forming a hydrophilic subphase. The regions around the perfluorinated backbone form a hydrophobic subphase. The segregation morphology is generally thought to be irregular; its scale is largely determined by the solvent content. The size of hydrophilic aggregates unlikely exceeds 100 Å.[50] Transport within the hydrophilic subphase is limited by the solvent motion between the aggregates. In block copolymers built of hydrophilic (e.g., sPS) and hydrophobic (e.g., polyolefin) blocks, the segregation scale is determined by the block length.[50] Block ionomers may segregate into various regular (lamellar, hexagonal, or cubic) and irregular morphologies.[51] The structure of individual hydrophilic blocks is more uniform than the structure of hydrophilic aggregates in perfluorosulfonate polymers. This enables rough predictions of the membrane morphology based on the block length and sorption data, which is not possible for hydrated perfluorosuflonate ionomers of Nafion type.

In this paper, we explore the specifics of solvation of the hydrophilic blocks of block copolymer membranes, such as sulfonated styrene-olefin triblock copolymers, in polar solvents by means of classical MD simulations. As a typical and practically relevant example, we model the interactions of individual sPS fragments with water, nerve agent simulant DMMP, and water-DMMP binary mixture with $K^+$, $Ca^{2+}$, and $Al^{3+}$ counterions. We analyze the influence of the solvent composition and the counterion on the polymer conformation and the local structure of the solvation shells. The structural and transport properties of sPS are compared to those of Nafion.

The structure of the paper is as follows. The systems considered and the simulation methods are described in Sec. II. In Sec. III, we discuss the molecular force fields employed in the simulations. The force field parameters for Nafion, water, DMMP, and counterions were taken from the literature. The force field for sPS has been developed specifically for this simulation using DFT optimization. The simulation results are presented and discussed in Sec. IV. First, we analyze the natural conformations of representative fragments of sPS blocks in vacuum and determine the characteristic torsion angles in the *trans* and *gauche* sequences. These conformations serve as references in the further analysis of solvation effects. Second, we study how the interactions with solvent and counterions affect the backbone conformation and stiffness. We show that the replacement of potassium or calcium by aluminum leads to a significant increase in salt absorption by sPS. Another interesting finding is that both sPS and Nafion are deplasticized in the presence of DMMP due to the increasing backbone stiffness. Third, we study in detail the solvation of sulfonate groups and find significant differences for sPS and Nafion. The specifics of the solvent local distribution around the sulfonate group are demonstrated with pair correlation functions and three-dimensional images of solvation shells, which form either symmetric (for $PhSO_3^-$ group of sPS) or asymmetric (for Nafion sidechain) clouds. We show that the solvation in a water-DMMP mixture is characterized by a two-layer solvation shell with a pronounced local separation of water and DMMP. Main conclusions are summarized in Sec. V.

## II. SYSTEMS AND METHODS

### A. Sulfonated polystyrene fragments, counterions, and solvents

Tactic sPS fragments were composed of 10 and 20 monomer units. Each fragment was terminated with a methyl group at one end and a $PhSO_3^-$ group at the other end. The sulfonation was 100%, i.e., the sulfonate group was attached to every phenyl in *para* position. We assumed a random order of substitutes at aliphatic carbons, to which the phenyl groups were bound, since this order is not controlled in polystyrene synthesis. To explore the interactions of sPS in a hydrophilic subphase of swollen triblockcopolymer membranes, we considered the solvation of sPS fragments in water, DMMP, and water-DMMP 1:1 and 2:1 (by volume) binary solvents. Counterions studied experimentally in Ref. 52 were considered: potassium ($K^+$), calcium ($Ca^{2+}$), and aluminum ($Al^{3+}$) (see Table I). To preserve the electroneutrality in the systems with $Al^{3+}$ counterion, three $Al^{3+}$ ions and one $K^+$ were added to 10-monomer fragments. This ratio roughly mimics the actual situation in cation-substituted sPS, since the exchange capacity of both sPS and Nafion membranes to aluminum cation never reaches 100%.[52]

For comparison, we also modeled four-unit tetrafluoroethylene-perfluoro-3,6-dioxa-4-methyl-7-octenesulfonate oligomers (typical fragments of Nafion polymer, similar to those modeled in Ref. 2) with $K^+$ counterion in pure DMMP, since this system was not reported previously. Neighboring sidechains were separated by 18 $CF_2$ groups, which corresponds to the equivalent polymer weight of 1165. In each simulation, we introduced the number of solvent molecules to achieve the approximate cell volume of $2.7\times10^4$ Å$^3$ (box size of 30 Å) with 10-monomer sPS and Nafion, and $6.4\times10^4$ Å$^3$ (box size of 40 Å) with 20-monomer sPS.

### B. Simulation techniques

For reference quantum minimization, we employed the restricted Hartree–Fock (RHF) method with 6-31g** basis set and B3LYP exchange-correlation functional. All minimizations were done using the Baker–Pullay eigenvector following optimization algorithms[53] implemented in the PQS *ab initio* software package from Parallel Quantum Solutions on an eight-processor LINUX cluster.[54] The models of sPS and Nafion fragments were constructed and optimized using the MATERIALS STUDIO package from Accelrys.[55] The conjugate gradient method with the maximum atomic displacement of 0.1 Å was used for minimization. MD simulations were carried out at $T=303$ K and 1 atm. Lennard-Jones (LJ) and electrostatic potentials were cut off at 14 Å. To account for long-range electrostatic interactions, the Ewald summation was applied. The temperature and pressure were maintained by the Nose–Hoover thermostat.[56,57] The equa-

TABLE I. The list of systems modeled.

| Fragment[a] | Monomers | Counter ions | Solvent | | | Averaging time (ns) |
|---|---|---|---|---|---|---|
| | | | Composition | $N_{H2O}$[b] | $N_{DMMP}$[b] | |
| SPS | 10 | 10 $K^+$ | Water | 750 | | 4 |
| SPS | 20 | 20 $K^+$ | Water | 2000 | | 6 |
| sPS | 20 | 20 $K^+$ | DMMP | | 420 | 6 |
| sPS | 10 | 10 $K^+$ | Water+DMMP (1:1 vol) | 375 | 53 | 4 |
| sPS | 10 | 5 $Ca^{2+}$ | Water | 750 | | 4 |
| sPS | 10 | 5 $Ca^{2+}$ | Water+DMMP (1:1 vol) | 375 | 53 | 4 |
| sPS | 10 | 3 $Al^{3+}$+$K^+$ | Water | 750 | | 4 |
| sPS | 10 | 3 $Al^{3+}$+$K^+$ | Water+DMMP (2:1 vol) | 475 | 35 | 4 |
| Nafion | 4 | 4 $K^+$ | DMMP | | 420 | 4 |

[a]The sequence of substitutes at asymmetric atom was RRSSRSSRRSR in 10-mers and RRSSRSSRRSRRRSSRSSRRSR in 20-mers from the "head" (terminal methyl group); the seniority sequence of the substitutes is head, tail, phenyl, hydrogen.
[b]Number of molecules of that component.

tions of motion were solved by the double-time-step Tuckerman[58] scheme, with the fast-fluctuating forces integrated with a 0.2 fs time step and slower fluctuating forces integrated with a 2 fs time step. All MD simulations were performed using the MDYNAMIX5.0 software package.[59,60] The GOPENMOL program[61] was used for the visualization of the results.

In the initial configuration of MD simulation, the fragment molecule was placed in a cavity, surrounded by solvent molecules that were arranged as a face centered cubic lattice at a low density of 0.05 $g/cm^3$. During the first 70 ps of the simulation trajectory, the cubic simulation box was gradually compressed until the desired density of 0.8 $g/cm^3$ was reached. The compression was followed by a 40 ps *NVT* simulation with the oligomer molecule kept rigid, to establish a preliminary equilibrium in the solvent. Then the simulation was carried out in the *NPT* ensemble at atmospheric pressure. The total length of the simulations was 5 ns for Nafion and 10-monomer sPS fragments, and 7 ns for 20-monomer sPS fragments (Table I). Every 100 fs the configuration of the whole system was saved for further analysis, which was performed with the TRANAL program of the MDYNAMIX 4.4 package.[59,60]

## III. MOLECULAR FORCE FIELDS

### A. Sulfonated polystyrene

MD simulations of arenes and polyethylene have been reported in the literature; both all-atom and united-atom molecular force fields have been developed for this class of molecules.[62–64] However, no suitable force fields were developed for sulfonated arenes, and we had to calculate a few new parameters specific to this class of systems. The total potential energy of the system was represented as a sum of LJ, Coulombic, covalent bond stretching, angle bending, and dihedral energy terms. United-atom LJ from a force field[62] was employed to describe the van der Waals interactions. The LJ parameters for the sulfonate group were taken equal to those in Nafion.[3] In order to assign the point charges to the atoms, we performed a RHF minimization of benzenesulfonate anion $C_6H_5SO_3^-$ and 2,4-diphenylpentane. Point charges were assigned to the atoms according to the orbital population analysis given in Table II. The negative charges on the sulfonate group oxygens were slightly stronger than those used previously in Nafion simulations. All covalent bonds were kept rigid using the SHAKE algorithm,[65] and the contribution to the potential energy coming from the bond stretching was omitted in this work. The equilibrium bond distances for the hydrocarbon backbone and phenyl groups were taken according to the TRAPPE force field;[62] the lengths of the C—S and S=O bonds were taken equal to those in minimized Ph-$SO_3^-$ structure. Covalent angle stretching was described by the simple harmonic potential $U_{\text{angle}}(\theta) = \frac{1}{2}K_\theta(\theta-\theta_0)^2$. For aliphatic backbone and benzene rings, we used the parameters from Ref. 62. In order to evaluate the rigidity of the covalent CCS, CSO and OSO angles, we performed a RHF minimization of benzenesulfonate ion with PQS *ab initio*.[54] Then, the parameters of the bending potentials were fitted to the directions and oscillation frequencies of sulfur and oxygen atoms. The parameters are given in Table II. The torsion angles of the hydrocarbon backbone were also taken from Ref. 62. The phenyl rings were kept rigid using out-of plane "improper" torsion potential functions in the standard harmonic form $U_{\text{impr}}(\phi) = \frac{1}{2}K_{\text{impr}}(\phi-\phi_0)^2$. The CCSO torsion that determines the rotation of the sulfonate group around the CS bond is of special interest. Benzenesulfonate ion has two major conformers: one has a *cis*-CCSO angle (one of the oxygens is located in the benzene ring plane) and the other has a straight CCSO torsion angle (one of the CCSO planes is perpendicular to the benzene ring, the other two form 31.5° angles with the ring plane). The latter is 0.16 kJ/mol less stable than the former. We fitted the parameters of the standard OPLS potential for torsion angles

$$U_{\text{tors}}(\theta) = \tfrac{1}{2}(1 + K_1\cos\theta) + \tfrac{1}{2}(1 - K_2\cos 2\theta) + \tfrac{1}{2}(1 + K_3\cos 3\theta) + \tfrac{1}{2}(1 - K_4\cos 4\theta)$$

to the energy difference between the conformations. The parameters obtained are presented in Table II. The united-atom force field for Nafion was taken from Ref. 3.

TABLE II. Parameters of the force field.

| Point charges, electrons | | | | | |
|---|---|---|---|---|---|
| CH3 | 0 | CH2 | 0 | CH | 0 |
| CB1 | −0.03 | CG2(5) | −0.02 | CB3(4) | −0.23 |
| CB4 | −0.230 | S | 1.755 | O | −0.75 |

| Counterions | $\sigma$ (Å) | $\varepsilon$ (kJ/mol) | Reference |
|---|---|---|---|
| $K^+$ | 3.36 | 0.568 | 66 |
| $Ca^{2+}$ | 2.44 | 0.5 | 77 |
| $Al^{3+}$ | 3.95 | 0.505 | 68 |

| Bonds | $K$ (kJ/mol/Å) | $r_0$ (Å) |
|---|---|---|
| $C_B$—S | 1400 | 1.85 |
| S—O | 2260 | 1.66 |

| Covalent angles | | | CCSO dihedral parameters | |
|---|---|---|---|---|
| Angle | $\theta_0$ (deg) | $K$ (kJ/mol/rad$^2$) | (kJ/mol/rad$^2$) | |
| CSO | 103.8 | 235 | $K_1$=3.1 | $K_2$=−9.4 |
| OSO | 114.8 | 421 | $K_3$=5.8 | $K_4$=0 |

| Improper torsion[a] | $K_{impr}$ (kJ/mol/rad$^2$) | $\phi_0$ (deg) |
|---|---|---|
| $C_B$—$C_B$—$C_B$—$C_B$ | 400 | 0 |
| $C_B$—$C_B$—$C_B$—$X$ | 400 | 180 |
| $X$—$C_B$—$C_B$—$X$ | 400 | 0 |

[a]$C_B$: an aryl carbon; $X$: a substitute.

### B. Counterions and solvents

Counterions were modeled as charged LJ centers. The LJ parameters for $K^+$ and $Ca^{2+}$ counterions were taken from Refs. 66 and 67, respectively. For $Al^{3+}$ cation, we simply used the LJ parameters from a generic universal force field.[68] Central potentials of LJ type cannot adequately describe the interactions of the aluminum ion with water and DMMP, which forms coordination compounds with water, such as the $[Al(H_2O)_6]^{3+}$ complex (the energy minimum for the interaction of $Al^{3+}$ ion with water corresponds to the distance of 1.76 Å between the metal and oxygen atoms according to Ref. 69 and our own DFT calculations). However, the LJ model is capable of reproducing important features of the systems under consideration, which are related to a general behavior of a trivalent cation capable of associating with the sulfonate groups. Water was modeled using SPC/E rigid model.[70] The molecular force field for DMMP was developed in our earlier work.[3]

## IV. RESULTS AND DISCUSSION

### A. Local conformations of hydrocarbon backbone

To explore "natural" conformations of the backbone, we identified characteristic conformers of 2,4-diphenylpentane (Fig. 1), which was chosen as a representative fragment of the sPS block. The second purpose of these molecular mechanics was to test the performance of the TRAPPE force field, the parameters of which were fitted to the thermodynamic properties of liquid alkanes and arenes rather than to conformations of individual complex molecules. 2,4-diphenylpentane is a symmetric substituted alkane that has two asymmetric carbons: $C_2$ and $C_4$ atoms have four different substitutes each. As a result, the alkane has two different isomers with different conformations: for example,

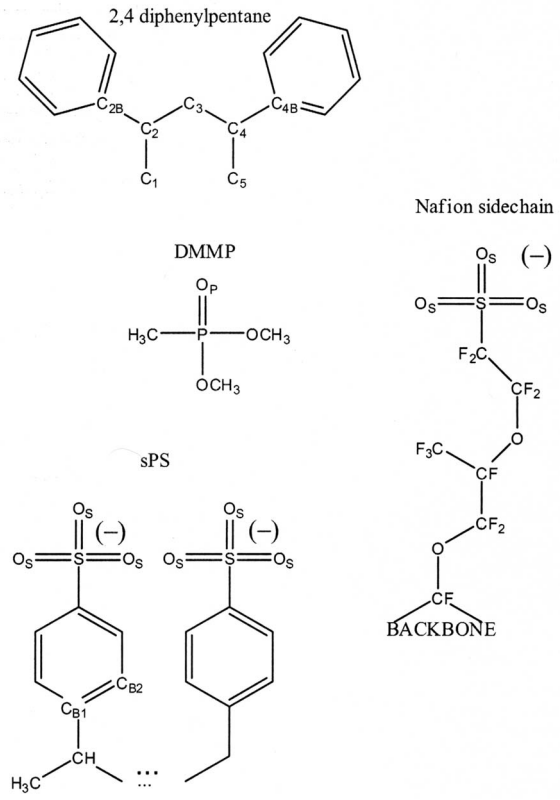


FIG. 1. Atom denotations in the compounds considered in the paper.

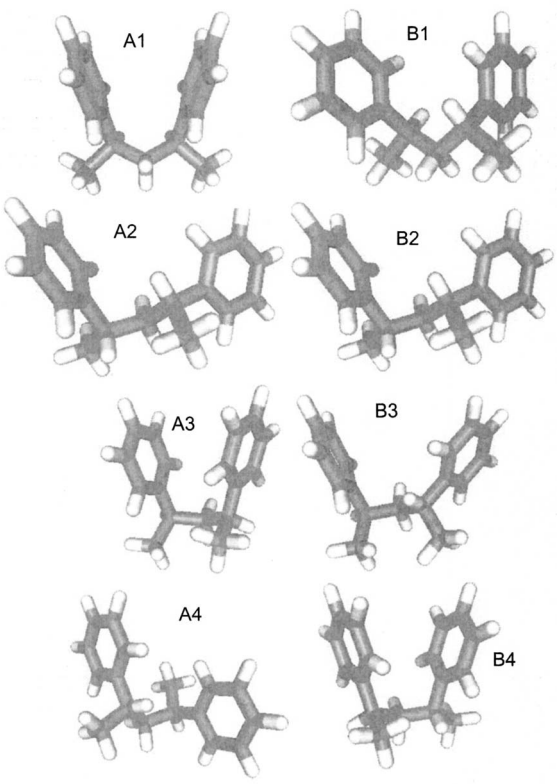


FIG. 2. Conformers of 2,3-diphenylpentane optimized in RHF with 6-31g$^{++}$ basis, B3LYP exchange-correlation functional. Left: isomer A; right: isomer B.

conformations depicted in Figs. 2(A1) and 2(B1) are different, asymmetric, and they cannot be obtained from each other by any sequence of internal rotations or mirror imaging; this can only be done by changing the substitute order at $C_2$ and/or $C_4$ carbons (in this way they are similar to enantiomers). Figure 2 depicts four major conformations for each isomer. We discern the conformations by two factors: (1) the elongation of the backbone that is determined by $C_1-C_2-C_3-C_4$ and $C_2-C_3-C_4-C_5$ torsion angles (for atoms denotation, see Fig. 1) and (2) the distance between the benzene rings determined by $C_{2B}-C_2-C_3-C_4$ and $C_{4B}-C_4-C_3-C_2$ torsions for each pair of the main torsion angles of the aliphatic backbone. The main torsion angles and energies are also given in Table III. The difference between the conformer reaches 26 kJ/mol for isomer A and 21 kJ/mol for isomer B. The locations of the benzene rings with respect to each other are qualitatively different for the two isomers. In both more stable conformations of isomer A [Figs. 2(A1) and 2(A3)], the benzene rings are almost parallel; these conformations are possibly stabilized by the $\pi$-$\pi$ interactions between the rings. They correspond to *trans-trans* (most elongated) and *gauche-gauche* (least elongated) conformations of the aliphatic backbone. On the other hand, for isomer B, the "folded" conformations with the phenyl group parallel to each other are less stable; the "extended" (more stable) conformations have *trans-trans* and *trans-gauche* pairs of the main angles.

TABLE III. Torsion angles and energies of main conformers of 2,4-dipenylpentane shown in Fig. 2. Two isomers differ by the order of substitutes at 2,4-asymmetric carbons.

| Conformer | | Torsion angles (deg) | | | | $E-E_0$ (kJ/mol) |
|---|---|---|---|---|---|---|
| | | C1—C2—C3—C4 | C5—C4—C3—C2 | C2B—C2—C3—C4 | C4B—C4—C3—C2 | |
| A1 | B3LYP | 158.8 | 158.8 | −76.1 | −76.1 | 0 |
| ttgg | TRAPPE | 167.4 | 167.4 | −67.8 | −67.8 | 0 |
| A2 | B3LYP | −161.6 | 71.6 | −74.0 | −58.9 | +1.0 |
| tggg | TRAPPE | −172.8 | 67.2 | −70.8 | −61.1 | +2.3 |
| A3 | B3LYP | 95.7 | 68.9 | 139.6 | −60.8 | +4.2 |
| ggtg | TRAPPE | 104.2 | 65.4 | 151.0 | −59.2 | +2.9 |
| A4 | B3LYP | 80.3 | 49.8 | 52.5 | 82.7 | +26.6 |
| gggg | TRAPPE | 66.1 | 54.3 | 56.8 | 80.0 | +33.0 |
| B1 | B3LYP | 172.7 | 172.7 | −62.1 | −62.1 | 0 |
| ttgg | TRAPPE | 173.3 | 173.3 | 58.7 | 58.7 | 0 |
| B2 | B3LYP | −48.9 | 169.5 | 82.5 | −65.9 | +21.2 |
| gtgg | TRAPPE | −54.2 | 173.3 | 77.4 | −64.6 | +17.4 |
| B3 | B3LYP | −62.8 | 97.1 | 66.9 | −138.2 | +19.4 |
| gggg | TRAPPE | 63.7 | 101.8 | 60.4 | −144.5 | +21.1 |
| B4 | B3LYP | 176.6 | 64.6 | 59.1 | 170.0 | +2.7 |
| tggt | TRAPPE | 176.5 | 63.3 | 57.8 | 174.4 | +4.6 |

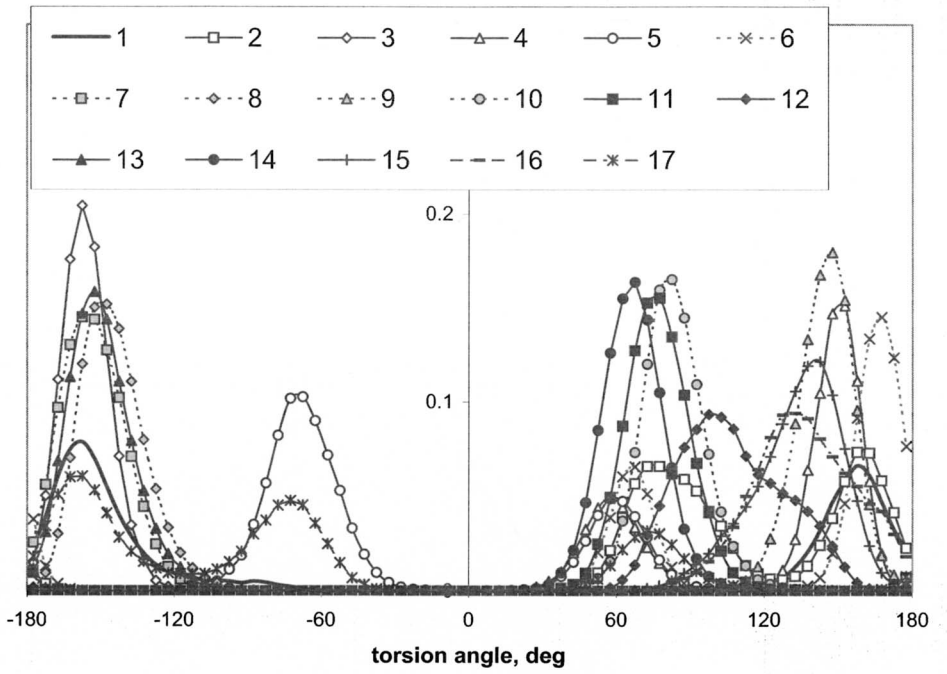


FIG. 3. The distributions of the aliphatic backbone dihedral angles in sPS 10-mer in water with $K^+$ counterion. The number on the legend show the number of the torsion in the aliphatic chain starting from the terminal $CH_3$ group: the backbone of the oligomer consists of 20 carbon atoms and 17 C–C–C–C dihedral angles.

Thus, we may conclude that the configuration and flexibility of the polymer depend substantially on the order of substitutes at the carbons, to which the phenylsulfonate groups are bonded. In this work, the sPS fragments have a random order of substitutes at each atom; therefore, both conformation types should be present. The sPS backbone is supposed to favor *trans* backbone angles although Table II shows that the angles are distorted considerably from the "normal" positions of 180° for *trans* and 60° for *gauche* configurations. The TRAPPE force field reproduces the conformations of 2,4-diphenylpentane well. All conformations are clearly identified and their relative stability is reproduced with very reasonable precision (Table III).

## B. Polymer-solvents interactions

### 1. Backbone conformations and stiffness

Solvated molecules do not have to repeat the conformations they exhibit in vacuum, especially in the presence of strong electrostatic interactions of sulfonate groups with water and counterions. In our simulations, aliphatic torsion angles exhibited distorted *trans* conformations predicted by the RHF optimization (Sec. IV A). For example, Fig. 3 shows the distribution of torsion angles of the aliphatic backbone of 10-monomer sPS fragments in water with a potassium counterion. The number in the legend shows the particular angle on the backbone; dihedral angles are numbered starting from the terminal $CH_3$ group (Fig. 1). The angle distribution shows preference to A1, A2, and B4 conformations of the backbone aliphatic chain (see also Table III and Fig. 2), for which the distorted *trans* ($\pm 150° - 170°$) and regular ($\pm 60$ deg) *gauche* angles are typical. However, a number of less stable conformations with normal *trans* torsions (typical for B1 conformer) were also present. The backbone was rather stiff: most torsion angles experienced not more than one transition within the entire 4 ns simulation period. On average, 0.2 transitions per 1 ns was detected in 10-monomer sPS fragments with water as a solvent and $K^+$ as counterion.

### 2. Effect of the counterion

It is expected that the counterion may substantially influence the conformations and flexibility of the sPS backbone. We did not observe any visible change of flexibility and conformations when $K^+$ counterion was replaced by $Ca^{2+}$. However, the sPS backbone behavior with $Al^{3+}$ was quite distinct. Figure 4 shows the intramolecular radial distribution function (RDF) for sulfur atoms attached to neighboring phenyl rings (intramolecular RDF is the probability distribution of finding the two atoms at a certain distance from each other). The first peak at 4–7 Å corresponds to folded conformations, that is, it is typical for conformations

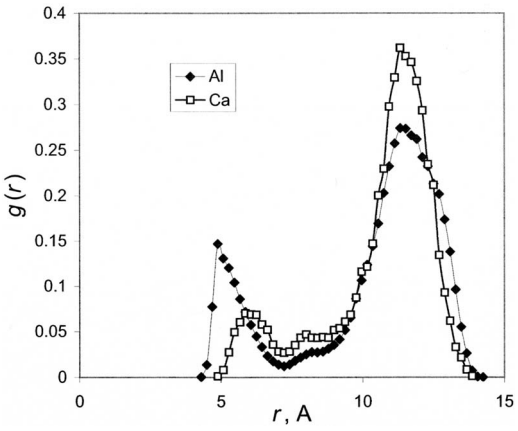


FIG. 4. Intermolecular RDFs between the sulfur atoms bonded to the neighboring phenyl groups of 10-monomer sPS oligomer with $Ca^{2+}$ and $Al^{3+}$ counterions.

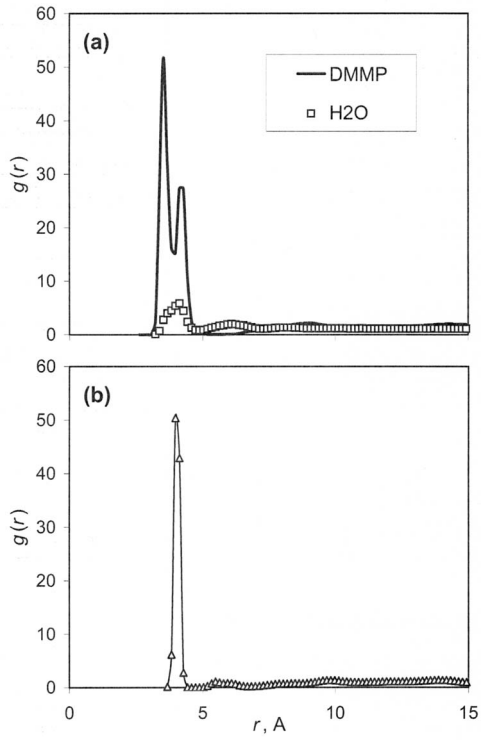


FIG. 5. RDF between the sulfur of the sulfonate group and the counterions in solutions of 10-monomer sPS fragments. (a) $K^+$ counterion in water and DMMP. (b) $Al^{3+}$ counterion in water.

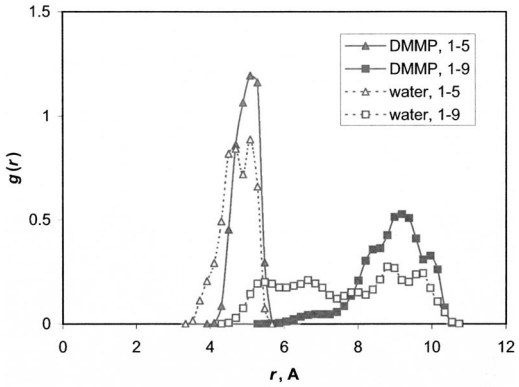


FIG. 6. Intramolecular RDFs for sPS 20-monomer oligomer in DMMP (closed symbols) and water (open symbols). The RDF is the average of all pairs of aliphatic chains with even numbers (i.e., the backbone carbons that phenyl rings are attached to) separated by 4 (1–5 neighbors) and 8 (1–9 neighbors). It is clear that the oligomer is stiffer in DMMP than in water.

(A1), (A4), (B3), and (B4) in Fig. 2. The second peak is broad. It corresponds to extended conformations (A2, A3, B1, and B2 is Fig. 2). For example, the distance between the neighboring sulfur atoms is 12 Å in conformation B2. Extended conformations prevail; however, when the $Ca^{2+}$ counterion is replaced by $Al^{3+}$, the fraction of the folded conformations approximately doubles and the first peak shifts from 6 to 4 Å. We attribute the change in conformations to the different behaviors of counterions. Both $K^+$ and $Ca^{2+}$ are mostly dissociated from the sulfate groups, the $Al^{3+}$ ion is associated, which is demonstrated by sulfur-counterion RDFs for $K^+$ and $Al^{3+}$ shown in Fig. 5 (the *intermolecular* RDF is the local concentration of atom *i* at a certain distance *r* from atom *j*, which is related to the average concentration of the former). The RDFs for $K^+$ and $Ca^{2+}$ counterions are typical for liquid solutions; the RDF for $Al^{3+}$ counterion shows two very high peaks corresponding to the counterion location either in the "palm" of the sulfonate group or on the periphery between two oxygens. The integration of the RDF shows a 98% probability of finding an $Al^{3+}$ counterion within 5 Å vicinity of the sulfur atom. This has a double effect on the conformation: (i) because three sulfonate groups are needed to neutralize a single $Al^{3+}$ counterion, strong electrostatic forces cause a distortion of the backbone; (ii) counterion dissociation critically alters the sidechain solvation by solvent molecules, since they interact with an anion rather than with an effective cation or dipole. $Al^{3+}$ ions surrounded by three sulfonate groups were observed rarely, because the electrostatic forces are not sufficient to overcome the energy barriers needed to fold a single backbone fragment to such an extent. In the hydrophilic phase of the bulk material, the neutralization is more readily achieved, because any ion may be surrounded by sulfonate groups belonging to different chains. Nevertheless, the gain in torsion energy may be quite significant. This effect explains why a sPS with trivalent counterions exhibits a notable osmotic uptake of salt solutions:[52] the extra salt resolves the need for counterion neutralization.

### 3. Effect of the solvent

In pure DMMP, the counterions are always associated with sulfate groups, as DMMP is an inferior solvent for the counterions as compared to water (for RDFs for $K^+$ with sulfur is shown in Fig. 5). In general, DMMP makes the backbone much stiffer. For example, the backbone of 10-monomer fragment with $K^+$ counterion showed a 0.1 transition per aliphatic bond per 1 ns in pure DMMP, which is twice as less often as in water. Figure 6 displays the intramolecular distribution functions between the backbone aliphatic carbons separated by four and eight covalent bonds. The RDFs show that the predominance for the *trans* configurations of the backbone is much stronger in DMMP, where the RDF for the atoms separated by eight bonds shows a distinct peak corresponding to 9.1 Å, which is nearly twice the distance for the peak of the RDF for carbons separated by four covalent bonds. A very different situation is observed in water, where RDFs show a variety of conformations. This observation agrees with the practical use of DMMP as deplasticizer for polymers.[71–73] This deplasticizing effect is most visible for Nafion. Both backbone and sidechain flexibilities were less pronounced than in water, methanol, or binary mixture modeled in Refs. 2 and 74. Even in water-DMMP 1:1 vol binary solvent, the deplasticizing effect of DMMP is quite pronounced: the backbones of sPS fragments were generally stiffer than in pure water. It is natural, since the backbone is surrounded by DMMP and only sulfonate groups and counterions are mostly solvated by water.

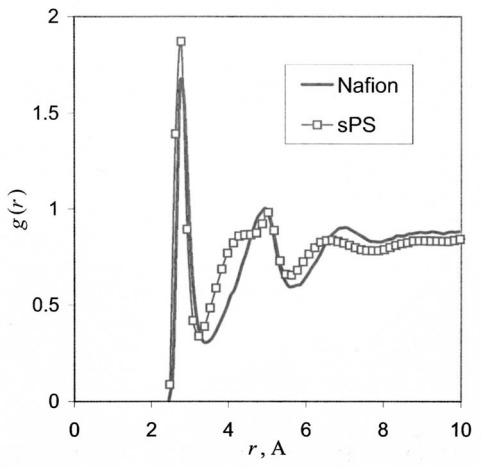


FIG. 7. RDF for oxygens of sulfonate groups and water in aqueous solutions of 10-monomer sPS oligomer and four-unit Nafion oligomer with $K^+$ counterion.

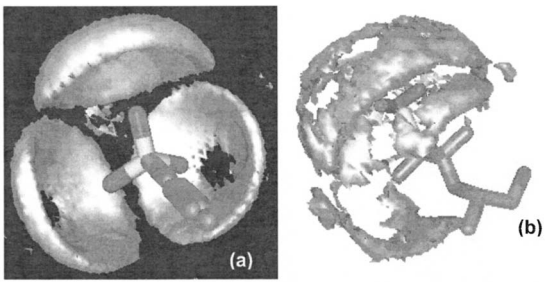


FIG. 8. SDFs of water oxygens around the phenylsulfonate group of (a) sPS and (b) Nafion sidechain in aqueous solutions with $K^+$ counterion. The sticks show the position of the atoms of the phenyl group averaged in a coordinate system rigidly attached to two S–O vectors; gray clouds show the locations where the average local density of water oxygens is 2.5 or more times greater than the average.

### C. Solvation of the sulfonate groups

#### 1. Solvation in water

As was described in detail in Refs. 2 and 74, water intensively interacts with sulfate groups via hydrogen bond donation. In this section, we analyze the difference between water interaction with the sulfonate groups of Nafion and sPS. Figure 7 shows the RDFs for oxygen atoms of water and those of sulfonate groups of the two polymers. The two RDFs are very similar. The first peak of the RDF is observed at about 3 Å, which corresponds to the oxygens of water molecules that form hydrogen bonds to the sulfonate group[2,74] and is somewhat higher in sPS solution. The geometrical analysis for hydrogen bonding similarly [a bond is formed if the distance between the donor and the acceptor oxygens is below 3.4 Å and the OHO angle exceeds 120° (Refs. 39 and 75)] showed 5.4 hydrogen bonds for the sulfonate group (with $K^+$ counterion), compared to 5.1 obtained in Ref. 2 (it should be noted that the $Na^+$ cation was considered in Ref. 2). The hydrogen bond lifetimes can be compared on the basis of the characteristic times of water molecules residing near the oxygens of sulfonate groups. We assumed that the residence of a water molecule at a certain sulfonate group is established when the distance between two oxygen atoms belonging to solvent molecules and an oxygen of a $SO_3^-$ group remained shorter that 3.4 Å within 2 ps. The residence was considered terminated when this distance exceeded 3.55 Å or when it remained larger than 3.4 Å within 2 ps.[2,39,75] The residence time estimate was based on the assumption that the probability of a hydrogen bond to be destroyed within time $t$ can be presented as $1-a\exp(-bt)$. Unlike the hydrogen bond numbers, the residence times do not involve the OHO angle as a criterium; however, since most of the stable contacts between negatively charged oxygen atoms originate from hydrogen bonds, the residence times give valuable information on the hydrogen bonding dynamics. The hydrogen bonds between water and sPS sulfonate groups appeared more stable than between water and Nafion sidechain [11.4 vs 8.3 (Ref. 2)]; however, the difference is not significant. In both cases, the hydrogen bond lasted over several rotation times of water molecule in the pure liquid [about 2.8 ps (Refs. 3 and 76)].

The RDF for sPS shows a small but pronounced and reproducible peak at about 5 Å, which indicates a strong anisotropic structuring. This structuring is demonstrated by spatial distribution functions (SDFs). SDF is a three-dimensional density profile, calculated in a reference coordinate system, rigidly attached to a part of the molecule of interest. For a better visualization, we built the reference coordinate systems on two OS vectors of each sulfonate group. The SFDs obtained for all side chains of each fragment were averaged.

Figure 8 shows the coordinates of the atoms of the $PhSO_3^-$ group in the reference system averaged over the simulation trajectory and the regions were the average local density of the water oxygens is 2.5 times as large as the average number density of the solvent. For comparison, we give a similar picture for Nafion (from Ref. 2). Because of the sulfonate group rotation around the C—S bond and the rigidity of the phenylsulfonate construction, the average locations on all carbons of the phenyl group as well as the aliphatic carbon, to which it is bonded, all fall onto the same straight line (Fig. 9). In both Nafion and sPS solutions, the first solvation shell is clearly observed and the second solva-

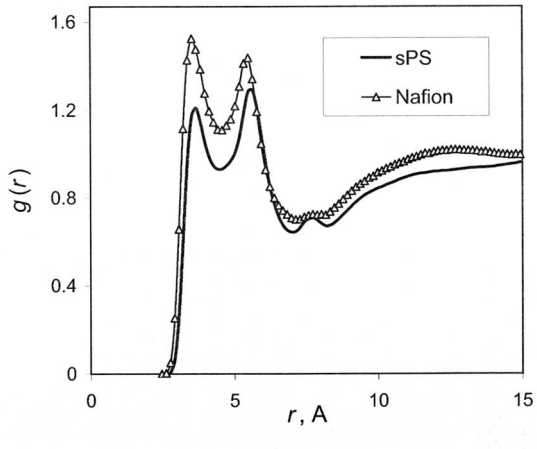


FIG. 9. Radial distribution functions between the oxygen atoms of sulfonate group of polymer fragments and $O_P$ oxygens of DMMP. Counterion is $K^+$.

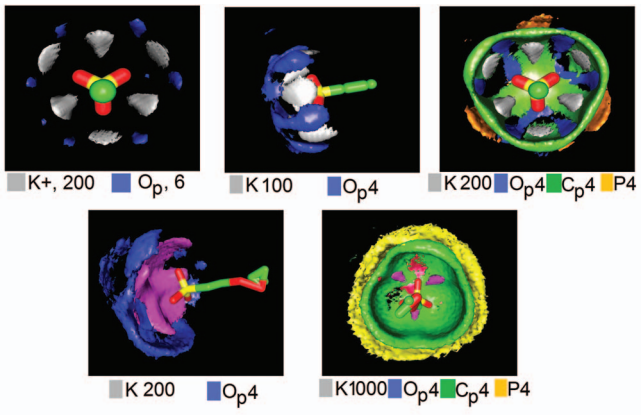


FIG. 10. (Color) SDFs of $K^+$ counterions and DMMP atoms (for denotations see Fig. 1) around the phenylsulfonate group of sPS (top) and Nafion sidechain (bottom). The sticks show the position of the atoms of the phenyl group averaged in a coordinate system rigidly attached to two S–O vectors. Different colors correspond to different atoms indicated under each image. The numbers are the relative intensities, i.e., the colored clouds show the areas where the average local concentration of a certain atom is higher than the average multiplied by the intensity level.

tion shell is hardly visible. It is clear that the solvation shell around the $PhSO_3^-$ group of sPS shows a strong anisotropic order, forming three distinct clouds corresponding to three oxygens of the sulfonate group. This behavior is somewhat similar to that observed in Nafion solution in methanol,[74] but the structuring in sPS-water systems is more pronounced.

### 2. Solvation in DMMP

A similar comparison between Nafion and sPS solvated in DMMP was performed. The RDF between sulfonate and $O_P$ oxygens (the oxygen of DMMP connected to the phosphorus by a double bond, Fig. 1) with $K^+$ counterion is shown in Fig. 9. (It appears that the RDF in Nafion is larger than in sPS within the entire range of distances shown; the only reason for that is the volume fraction of the polymer being different in the two simulations. This fact should therefore be ignored.) Again, the RDFs for Nafion and sPS are very similar. The counterion is associated; it is located in the vicinity of the group (Fig. 5), forming a very strong dipole. The dipoles of DMMP molecules are oriented, respectively, around the $SO_3^-K^+$ dipole. The first peak of the RDF is observed at a distance of 3.4 Å, which is close to that in water. The only situation we can suggest is that $O_S$, $O_P$, and $K^+$ atoms are all adjacent to each other. It is likely that the second peak corresponds to two other oxygens of the sulfonate group. For sPS in DMMP, the second peak is higher than the first peak, showing that the solvation shell of the phenylsulfonate group of sPS has a greater anisotropy than in Nafion.

This suggestion is confirmed by the SDFs of different atoms of DMMP and the counterion around the sulfonate group. The SDFs for the potassium counterion in sPS solution in DMMP show two distinct places where it could be located: either near an individual oxygen atom of the sulfonate group or at an equal distance to two atoms [Fig. 10(a)]. The preferential locations for the counterion around Nafion fragments are the same, but the overall range of possible locations is broader, and the cloud of preferential locations is smeared out [Figs. 10(a) and 10(d)]; in particular, the counterion may be located in the center between all three oxygens, which is not seen in the sPS solution.

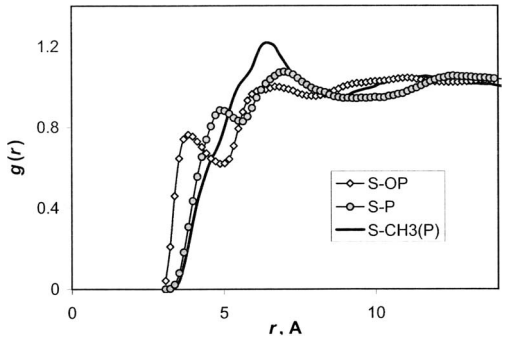


FIG. 11. Pair RDFs between DMMP and the phenylsulfonate group of sPS in DMMP-water 1:1 (vol) mixture. For atom denotations, see Fig. 1.

Overall, the anisotropic structure around the phenylsulfonate group of sPS is much more pronounced than around the Nafion sidechain. Figure 10(b) shows preferential locations of OP oxygens in the first shell, which form six identifiable clouds corresponding to the six locations of the counterion. The preferential locations of the phosphorus atom and the methyl group bound to phosphorus demonstrate a distinct orientation pattern, while the first solvation shells around Nafion, though very strong, are mostly isotropic (Fig. 11).

### 3. Solvation in water-DMMP binary mixture

As was shown in Ref. 3, the model Nafion sidechains introduced to the DMMP-water binary solution caused a segregation of the mixture into two subphases. A somewhat similar picture was observed in the solutions of sPS oligomers in the water-DMMP binary solvent. However, the segregation effect caused by the sPS oligomers was not that pronounced. DMMP surrounds the aliphatic backbone and the phenyl groups, while water mostly surrounds the sulfate groups and counterions. However, water cannot completely displace DMMP off the first solvation shell of both sulfate group and the anion. For example, Fig. 11 shows that the first peak is still present on the $O_P$–S RDF, which indicates the presence of DMMP in the first solvation shell of the sulfonate group; in the second shell (distance of 6 Å), the RDF is very close to 1, reflecting that the local composition of the second shell is the same as in the overall composition.

It should be noted that the hydrogen bonds between water and sulfonate groups in the mixture are more stable than in pure water, despite a mostly aqueous environment around the sidechains. We obtained the $O_W$–$O_S$ residence time of 15.8 ps, almost twice as long as for Nafion in pure water. The exact reason for this difference is unclear. It seems likely that larger and less mobile DMMP molecules surrounding the sulfonate groups solvated with waters constrict the motion of water and counterions, making the water molecules less mobile.

## V. CONCLUSIONS

We have performed a molecular dynamics simulation study of sPS fragments in water, nerve agent simulant DMMP, and their binary mixture in pursuit for a better understanding of interactions and dynamics in the hydrophilic subphase of solvated triblock copolymer membranes. We have established the force field parameters related to the sulfonate group by using *ab initio* optimization with the RHF method. We compare the specifics of solvation of sPS and Nafion.

We found a significant deplastification effect of DMMP both on sPS and Nafion polymer: the flexibility of the polymer backbone in DMMP and DMMP-water binary mixture is substantially reduced as compared to the backbone flexibility in pure water. A deplastification effect was also observed when a single-valent potassium or a two-valent calcium cation was replaced by a trivalent aluminum cation. The strong electrostatic forces in the last case caused strong conformation changes in sPS.

The solvent structuring around the sulfonate groups of sPS for both water and DMMP is similar to that of Nafion, but shows a much greater anisotropy. The solvation shell of water around the sulfonate group is determined by hydrogen bonding between water and the sulfonate group oxygens. Despite the apparent similarity in numbers and lifetimes of the hydrogen bonds, the spatial distribution functions show a distinct anisotropic structuring in the first solvation shell around the sulfonate groups in both water and DMMP, which is not observed in Nafion. We relate this changes to the lack of flexibility of the phenylsulfonate group (as compared to the Nafion sidechain) and the anisotropy of the phenyl ring.

The simulation of sPS fragments in the water-DMMP binary mixture showed a partial segregation of the solvent mixture with DMMP prevailing around the hydrocarbon backbone and water surrounding the sulfonate groups. Both water and DMMP were found in the first solvation shell of the counterion. The segregation is less pronounced in sPS than in Nafion, likely because of a smaller flexibility of the backbone and a shorter distance between the sulfonate groups in sPS. We expect that the hydrophilic subphase of the sulfonated triblock copolomer membranes swollen in water and DMMP will remain uniform at the scales smaller than 30 Å.

It is worth noting that the structural properties of sPS solutions obtained in this work (Fig. 6) can be employed for the development of a force field for mesoscale simulations of the hydrophilic phase of the triblock copolymer membranes using the concept of the mean force potential. Fitting the distribution functions for the backbone conformations, we have derived a coarse-grained model of sPS with the effective bead representing four styrene monomers and obtained the potential of mean force sPS in water and DMMP. These results will be published elsewhere.

## ACKNOWLEDGMENTS

This work was supported by the US Army Research Office Grant No. W911NF0410239 "Molecular Design of Triblock Copolymer Permselective Membranes." The authors are thankful to Dr. Nathan Schneider for stimulating discussions.

[1] E. Napadensky and Y. A. Elabd, "Breathability and selectivity of selected materials for protective clothing," ARLWMRD, Aberdeen, 2004.
[2] A. Vishnyakov and A. V. Neimark, J. Phys. Chem. B **104**, 4471 (2000).
[3] A. Vishnyakov and A. V. Neimark, J. Phys. Chem. A **108**, 1435 (2004).
[4] S. S. Jang and W. A. Goddard, J. Phys. Chem. C **111**, 2759 (2007).
[5] S. J. Paddison, L. R. Pratt, and T. A. Zawodzinski, J. New Mater. Electrochem. Syst. **2**, 183 (1999).
[6] S. J. Paddison and T. A. Zawodzinski, Solid State Ionics **115**, 333 (1998).
[7] S. Urata, J. Irisawa, A. Takada, S. Tsuzuki, W. Shinoda, and M. Mikami, J. Fluorine Chem. **126**, 1312 (2005).
[8] S. Urata, J. Irisawa, A. Takada, S. Tsuzuki, W. Shinoda, and M. Mikami, Phys. Chem. Chem. Phys. **6**, 3325 (2004).
[9] S. Urata, J. Irisawa, A. Takada, W. Shinoda, S. Tsuzuki, and M. Mikami, J. Phys. Chem. B **109**, 17274 (2005).
[10] S. J. Paddison, L. R. Pratt, and T. A. Zawodzinski, J. Phys. Chem. A **105**, 6266 (2001).
[11] S. T. Cui, J. W. Liu, M. E. Selvan, D. J. Keffer, B. J. Edwards, and W. V. Steele, J. Phys. Chem. B **111**, 2208 (2007).
[12] S. Yamamoto and S. A. Hyodo, Polym. J. (Tokyo, Jpn.) **35**, 519 (2003).
[13] A. Vishnyakov and A. V. Neimark, J. Phys. Chem. B **105**, 9586 (2001).
[14] E. Spohr, Mol. Simul. **30**, 107 (2004).
[15] D. Seeliger, C. Hartnig, and E. Spohr, Electrochim. Acta **50**, 4234 (2005).
[16] F. Meier and G. Eigenberger, Electrochim. Acta **49**, 1731 (2004).
[17] T. Li, A. Wlaschin, and P. B. Balbuena, Ind. Eng. Chem. Res. **40**, 4789 (2001).
[18] S. S. Jang, V. Molinero, T. Cagin, and W. A. Goddard, J. Phys. Chem. B **108**, 3149 (2004).
[19] S. S. Jang, S. T. Lin, T. Cagin, V. Molinero, and W. A. Goddard, J. Phys. Chem. B **109**, 10154 (2005).
[20] J. A. Elliott, S. Hanna, A. M. S. Elliott, and G. E. Cooley, Phys. Chem. Chem. Phys. **1**, 4855 (1999).
[21] P. Choi, N. H. Jalani, and R. Datta, J. Electrochem. Soc. **152**, E84 (2005).
[22] N. P. Blake, M. K. Petersen, G. A. Voth, and H. Metiu, J. Phys. Chem. B **109**, 24244 (2005).
[23] N. P. Blake, G. Mills, and H. Metiu, J. Phys. Chem. B **111**, 2490 (2007).
[24] C. Ayyagari, D. Bedrov, and G. D. Smith, Polymer **45**, 4549 (2004).
[25] S. Urata, J. Irisawa, A. Takada, W. Shinoda, S. Tsuzuki, and M. Mikami, J. Phys. Chem. B **109**, 4269 (2005).
[26] P. Commer, C. Hartnig, D. Seeliger, and E. Spohr, Mol. Simul. **30**, 755 (2004).
[27] S. Dokmaisrijan and E. Spohr, J. Mol. Liq. **129**, 92 (2006).
[28] E. Spohr, P. Commer, and A. A. Kornyshev, J. Phys. Chem. B **106**, 10560 (2002).
[29] A. Roudgar, S. P. Narasimachary, and M. Eikerling, J. Phys. Chem. B **110**, 20469 (2006).
[30] E. J. Lamas and P. B. Albuena, Electrochim. Acta **51**, 5904 (2006).
[31] D. Rivin, G. Meermeier, N. S. Schneider, A. Vishnyakov, and A. V. Neimark, J. Phys. Chem. B **108**, 8900 (2004).
[32] M. K. Petersen, F. Wang, N. P. Blake, H. Metiu, and G. A. Voth, J. Phys. Chem. B **109**, 3727 (2005).
[33] S. J. Paddison, Annu. Rev. Mater. Res. **33**, 289 (2003).
[34] A. Z. Weber and J. Newman, Chem. Rev. (Washington, D.C.) **104**, 4679 (2004).
[35] T. D. Gierke and W. Y. Hsu, ACS Symp. Ser. **180**, 283 (1982).
[36] T. D. Gierke, G. E. Munn, and F. C. Wilson, J. Polym. Sci., Polym. Phys. Ed. **19**, 1687 (1981).
[37] M. Eikerling, A. A. Kornyshev, and U. Stimming, J. Phys. Chem. B **101**, 10807 (1997).
[38] J. Ennari, M. Elomaa, and F. Sundholm, Polymer **40**, 5035 (1999).
[39] A. P. Lyubartsev and A. Laaksonen, J. Biomol. Struct. Dyn. **16**, 579 (1998).
[40] J. S. Duca and A. J. Hopfinger, Comput. Theor. Polym. Sci. **9**, 227 (1999).
[41] R. D. Groot, J. Chem. Phys. **118**, 11265 (2003).
[42] J. T. Wescott, Y. Qi, L. Subramanian, and T. W. Capehart, J. Chem. Phys. **124**, 134702 (2006).
[43] D. Y. Galperin and A. R. Khokhlov, Macromol. Theory Simul. **15**, 137 (2006).
[44] P. G. Khalatur, S. K. Talitskikh, and A. R. Khokhlov, Macromol. Theory

Simul. **11**, 566 (2002).
[45] D. A. Mologin, P. G. Khalatur, and A. R. Kholhlov, Macromol. Theory Simul. **11**, 587 (2002).
[46] N. Urakami and M. Takasu, Mol. Simul. **19**, 63 (1997).
[47] N. Korolev, A. P. Lyubartsev, A. Laaksonen, and L. Nordenskiold, Nucleic Acids Res. **31**, 5971 (2003).
[48] N. Korolev, A. P. Lyubartsev, and L. Nordenskiold, J. Biomol. Struct. Dyn. **20**, 275 (2002).
[49] N. Korolev, A. P. Lyubartsev, A. Laaksonen, and L. Nordenskiold, Biophys. J. **82**, 2860 (2002).
[50] I. Capek, Adv. Colloid Interface Sci. **118**, 73 (2005).
[51] X. Y. Lu, W. P. Steckle, and R. A. Weiss, Macromolecules **26**, 3615 (1993).
[52] N. S. Schneider and D. Rivin, Polymer **47**, 3119 (2006).
[53] J. Baker, J. Comput. Chem. **7**, 385 (1986).
[54] PQS, PQS *Ab Initio* Program Package Version 3.3, Parallel Quantum Solutions, Fayetteville, AR, 2004.
[55] I. Accelrys, CERIUS2, Accelrys Inc., San Diego, CA, 2000.
[56] S. Nose, Mol. Phys. **52**, 255 (1984).
[57] W. G. Hoover, Phys. Rev. A **31**, 1695 (1985).
[58] M. Tuckerman, J. Chem. Phys. **97**, 1990 (1992).
[59] A. P. Lyubartsev and A. Laaksonen, Comput. Phys. Commun. **128**, 565 (2000).
[60] A. Lyubartsev, MDYNAMIX, A Molecular Dynamics Program, Stockholm University, Stockholm, 2007 (http://www.fos.su.se/~sasha/mdynamix).
[61] L. Laaksonen, GOPENMOL, CRC, Finnish IT Centre for Science, Espoo, Finland, 2001 (http://www.csc.fi/gopenmol/).
[62] C. D. Wick, M. G. Martin, and J. I. Siepmann, J. Phys. Chem. B **104**, 8008 (2000).
[63] P. A. Gordon, J. Chem. Phys. **125**, 014504 (2006).
[64] V. A. Harmandaris, N. P. Adhikari, N. F. A. van der Vegt, and K. Kremer, Macromolecules **39**, 6708 (2006).
[65] W. F. vanGunsteren and H. J. C. Berendsen, Mol. Phys. **34**, 1311 (1977).
[66] K. Heinzinger, Physica B & C **131**, 196 (1985).
[67] T. Megyes, I. Bako, S. Balint, T. Grosz, and T. Radnai, J. Mol. Liq. **129**, 63 (2006).
[68] A. K. Rappe, C. J. Casewit, K. S. Colwell, W. A. Goddard, and W. M. Skiff, J. Am. Chem. Soc. **114**, 10024 (1992).
[69] A. Bakker, K. Hermansson, J. Lindgren, M. M. Probst, and P. A. Bopp, Int. J. Quantum Chem. **75**, 659 (1999).
[70] H. J. C. Berendsen, J. R. Grigera, and T. P. Straatsma, J. Phys. Chem. **91**, 6269 (1987).
[71] K. J. Calzia, A. Forcum, and A. J. Lesser, J. Appl. Polym. Sci. **102**, 4606 (2006).
[72] A. S. Zerda and A. J. Lesser, J. Appl. Polym. Sci. **84**, 302 (2002).
[73] A. S. Zerda and A. J. Lesser, Polym. Eng. Sci. **44**, 2125 (2004).
[74] A. Vishnyakov and A. V. Neimark, J. Phys. Chem. B **105**, 7830 (2001).
[75] A. Vishnyakov, G. Widmalm, J. Kowalewski, and A. Laaksonen, J. Am. Chem. Soc. **121**, 5403 (1999).
[76] J. Kowalewski and E. Kovacs, Z. Phys. Chem., Neue Folge **149**, 49 (1986).
[77] S. Marchand and B. Roux, Proteins: Struct., Funct., Genet. **33**, 265 (1998).